Rotational spectra and structures of Rg–C6H6–H2O trimers and the Ne–C6H6 dimer (Rg=Ne, Ar, or Kr)

E. Arunan, T. Emilsson, and H. S. Gutowsky

Citation: The Journal of Chemical Physics **101**, 861 (1994); doi: 10.1063/1.467738
View online: http://dx.doi.org/10.1063/1.467738
View Table of Contents: http://scitation.aip.org/content/aip/journal/jcp/101/2?ver=pdfcov
Published by the AIP Publishing

Rotational spectra and structures of Rg–C_6H_6–H_2O trimers and the Ne–C_6H_6 dimer (Rg=Ne, Ar, or Kr)

E. Arunan, T. Emilsson, and H. S. Gutowsky
Noyes Chemical Laboratory, University of Illinois, Urbana, Illinois 61801

(Received 14 December 1993; accepted 30 March 1994)

Rotational spectra of Rg–C_6H_6–H_2O isotopomers, where Rg=Ne, Ar, or Kr, have been observed with a Balle–Flygare Fourier transform microwave spectrometer. In these trimers the benzene is sandwiched between the rare gas and H_2O. Isotopic substitution and inertial analyses show that the Rg–C_6H_6 distance in the trimer is reduced by about 0.01 Å for Ne, Ar, and Kr compared to the corresponding distance in the Rg–C_6H_6 dimer. On the other hand, the c.m. (C_6H_6) to c.m. (H_2O) distance in the trimers is increased by only about 0.003 Å from its distance in the dimer. Symmetric top spectra of ^{20}Ne–C_6H_6 and ^{22}Ne–C_6H_6 were observed as an aid in the comparison. Hyperfine structure (hfs) and substitution analyses with HDO/D_2O containing isotopomers reveal that the $m=0$ and 1 states of H_2O in the trimer are virtually unchanged from those in the C_6H_6–H_2O dimer, including essentially free rotation. In addition, analyses are made of the root-mean square (rms) deviation for the benzene C_6 axis from the **a** axis in the dimers (~19 deg) and trimers (~21 deg) and of the displacement of the C_2 axis of the water from the **a** axis in the trimers (~37 deg).

I. INTRODUCTION

We recently reported[1] preliminary observations of the rotational spectrum for Ne–C_6H_6–H_2O, a symmetric top trimer in which C_6H_6 is sandwiched between Ne and H_2O. Here we give a detailed account of our studies on Ne–C_6H_6–H_2O as well as similar results for Ar–C_6H_6–H_2O and Kr–C_6H_6–H_2O. The trimers may be thought of as a composite of the Rg–C_6H_6 and C_6H_6–H_2O dimers, where Rg=Ne, Ar, or Kr. Of the dimers, rotational spectra have been reported for Ar–C_6H_6,[2] Kr–C_6H_6,[3] and C_6H_6–H_2O.[4,5] However, at the time of our initial work on the Ne–C_6H_6–H_2O sandwich,[1] the rotational spectrum of Ne–C_6H_6 was not yet available. So, for comparative purposes, we observed and analyzed rotational spectra for the ^{20}Ne–C_6H_6 and ^{22}Ne–C_6H_6 dimers, the result of which are included here.

The Rg–C_6H_6–H_2O trimer system is interesting for various reasons. It includes the weak Rg–C_6H_6 van der Waals interaction on one side of the benzene ring and the stronger C_6H_6–H_2O hydrogen bonding on the other side. Thus, studies of Rg–C_6H_6–H_2O trimers could not only improve our understanding of these two interactions but also shed some light on the effect of these interactions on one another. For example, Weber and Neusser reported rotationally resolved ultraviolet spectra[6] of Ar–C_6H_6–Ar in which they found the two Ar–C_6H_6 distances to be the same as that observed in the dimer, i.e., there is no third-body effect due to the weak Ar–C_6H_6 interaction. On the other hand, in linear trimers containing $(HCN)_2$, all involving H bonding, it was found that the distance between any two successive monomers was significantly shorter than the corresponding value in the dimer.[7,8]

The C_6H_6–H_2O dimer has attracted attention recently,[4,5,9,10] because studies of it can help clarify the hydrophobic interactions between C_6H_6 and H_2O in bulk.[11] Moreover, our results[4] on the low J rotational spectra of the C_6H_6–H_2O dimer exhibited several unusual features. The H_2O is virtually free to rotate internally, leading to a symmetric top ground-state ($m=0$) spectrum, even though the rigid dimer is an asymmetric top. Also, spectra were observed for the first excited internal rotation state ($m=1$) of the H_2O and D_2O isotopic species, where relaxation to the $m=0$ ground state is spin-forbidden.

It was found for the dimer[4] that the rotational spectra for both $m=0$ and $m=1$ states could be fitted to the following equation used by Fraser *et al.*[12] for the CF_3H–NH_3 dimer:

$$\nu=2(J+1)(B-D_{JK}K^2-D_{Jm}m^2-D_{JKm}Km-H_{JKm}K^2m^2) -4D_J(J+1)^3. \quad (1)$$

However, an independent fit of the $m=1$ lines showed that the fit could be improved significantly by replacing D_J in Eq. (1) with an m dependent term, $D_J-D_{JJm}m^2$. In the $m=1$ progression, the highest frequency line was missing at each $J\geqslant 1$ and then there was an odd line just above the $m=0$ symmetric top lines. We assigned this to be the missing $m=1$ line. Finally the H_2O/D_2O hyperfine structure observed for the $m=1$ state differs from predictions[9] based on a model in which the benzene and water rotate about coaxial C_6 and C_2 axes. Though most of these features are still not understood, observation of their counterparts in the trimers, as reported in this paper, is convincing evidence for their reality.

Benzene–rare gas clusters have been studied theoretically[13–16] and experimentally[2,3,6,17–20] as models for van der Waals interactions in aromatic systems and in dimers between two nonpolar units. Rotational spectra were obtained[2,3] for Ar–C_6H_6 and Kr–C_6H_6 to pinpoint their structures. However, initial attempts to observe the rotational spectrum for the Ne–C_6H_6 dimer by Bauder and co-workers were not successful.[14] Encouraged by our observations of the Ne–C_6H_6–H_2O trimer and by reliable rotationally resolved UV spectroscopy results[18] we observed the rotational spectra of ^{20}Ne–C_6H_6 and ^{22}Ne–C_6H_6. Later, we learned that Bauder's group had also observed the rotational spectrum of ^{20}Ne–C_6H_6.[21] Our results on the ^{20}Ne/^{22}Ne–C_6H_6 dimers

 0021-9606/94/101(2)/861/8/$6.00

give us an accurate intermolecular distance as well as the "tilt" angle, the rms deviation of the benzene C_6 axis from the **a** axis. Both of these serve as a useful basis for an extensive comparison of the properties for the dimers and trimers incorporating the three rare gases.

II. EXPERIMENT

Rotational spectra of the Rg–C_6H_6–H_2O trimers and the Ne–C_6H_6 dimer were observed with the Mark II Balle/Flygare Fourier transform microwave spectrometer.[22] The complexes were formed typically in first run neon with 1.5 to 2.0 atm backing pressure. The C_6H_6 and H_2O were added by bubbling 1% and 2% of the carrier gas through the liquids at ambient conditions. For Ar–C_6H_6–H_2O and Kr–C_6H_6–H_2O, some 5% to 10% of Ar/Kr was mixed with the carrier gas. The pulsed nozzle (General Valve) has a diameter of ~1 mm and was operated typically at 10 Hz. Sixteen microwave pulses were applied during each gas pulse. Polarizing microwave pulses of 0.3 μs were optimal for Rg–C_6H_6–H_2O trimers while 5–6 μs pulses were needed for the Ne–C_6H_6 dimers. Amplification of the microwave power improved the Ne–C_6H_6 signal by a factor of 20, though the signal could be seen without an amplifier.

The $J=0\rightarrow1$ transitions for Ne–C_6H_6–H_2O occur at frequencies (1.8 to 1.9 GHz) which are below our previous operating limit of 2280 MHz set by a transition reported[23] for ^{82}Kr–HC^{15}N. The problem is that at low frequencies the "Q" of the Fabry–Perot resonator deteriorates rapidly. As the wavelength increases the microwave beam waist becomes wide enough for energy to be lost from the edges of the mirrors. To prevent this loss, the mirrors were fitted with 8 in. wide, tight fitting aluminum sheet collars. With these in place, good sharp resonances were observed down to 1.7 GHz. We do not know whether the resonator itself functions at lower frequencies. Most of the microwave components in the system are rated only to 2 GHz and, at 1.7 GHz, are operating well outside their design limits.

Coupling of the resonator to the microwave source required modification for the lower frequencies. Extension downward of the frequency range with waveguides would be impractical because of the sheer size of low-frequency waveguides. A coupling accessory was built using 0.141 in. semirigid coaxial cable as shown in Fig. 1. For convenience it was designed so that it could be slipped through the existing X-band waveguide, simplifying the installation and removal. (W) is the waveguide which butts against the coupling iris (H) on the mirror (M). The microwave wave signal is coupled to or from the resonator by the antenna (A), made from two 1/4 wavelength pieces of silvered wire. The antenna is a balanced device which needs a "balun" transformer (B) to be properly connected to the unbalanced coaxial transmission line.

The balun transformer is simply a piece of 3/8 in. diameter brass rod with a 1/4 wave deep well at the output end. Although the dimensions of the antenna and balun are wavelength specific, good performance can be had over a range of more than one octave. Two couplers have covered the range from 1.7 to 8 GHz. Not shown on Fig. 1 are the provisions for accurately adjusting the distance between the antenna and the mirror. This allows adjustment of the coupling coefficient and makes it easier to obtain critical coupling to the resonator. Also not shown in Fig. 1 is a provision for rotating the coupler and antenna about the axis. By adjusting the rotation angle it is usually possible to get rid of spurious cavity ringing which sometimes overwhelms the molecular signal.

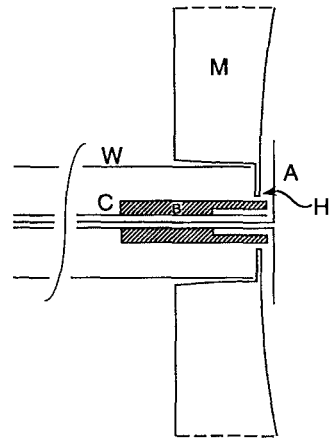

FIG. 1. Details of the coaxial coupler to the cavity. (M) is the mirror with a coupling hole (H) and (W) is the X-band waveguide. (A) is the antenna, fed by the semirigid coaxial cable (C), connected through the balun (B).

The search for Ne–C_6H_6–H_2O isotopomers was described in our preliminary communication.[1] The Ar–C_6H_6–H_2O and Kr–C_6H_6–H_2O spectra were predicted by assuming the trimer geometry to be the composite of the free Rg–C_6H_6 and C_6H_6–H_2O[4] dimers.[2–5] In the predictions both the Rg and the O atoms were assumed to be on the C_6 axis of the benzene. It was found that using a hypothetical C_{4v} H_2O molecule with 1/2 the H mass on each corner served as a good model for predicting symmetric top spectra of all the Rg–C_6H_6–H_2O isotopomers studied. Once the $m=0$ symmetric top transitions were observed, the $m=1$ lines for the lowest J were searched for with Eq. (1) as a guide. The higher J transitions were then predicted and observed.

The argon was obtained from Liquid Air. Neon and krypton were purchased from MG Industries. Fisher's reagent grade C_6H_6 was used. The $H_2{}^{18}O$ with 92.5% ^{18}O was obtained from Isotec, Inc. The D_2O (99.9% D) was obtained from Sigma and HDO was produced by mixing equal amounts of H_2O and D_2O in the bubbler.

III. RESULTS AND ANALYSIS

A. Rg–C_6H_6–H_2O sandwich trimers

1. Assignments and rotational constants

a. $m=0$ ground state. The ground-state, $m=0$ transitions could be fitted accurately for all three Rg–C_6H_6–H_2O trimers with the standard symmetric top equation[24]

$$\nu=2(J+1)(B-D_{JK}K^2)-4D_J(J+1)^3. \quad (2)$$

The frequencies observed for the parent isotopic species (Rg=^{20}Ne, ^{40}Ar, or ^{84}Kr) are listed in Table I. Some of the low J transitions for Kr–C_6H_6–H_2O were not well resolved

TABLE I. Observed frequencies (MHz) of rotational transitions for the parent Rg–C_6H_6–H_2O trimers in the $m=0$ state (Rg=^{20}Ne, ^{40}Ar, or ^{84}Kr).

$J \rightarrow J'$	K	Ne–C_6H_6–H_2O	Ar–C_6H_6–H_2O	$J \rightarrow J'$	K	Kr–C_6H_6–H_2O
0 1	0	1918.6911	···	4 5	3	4677.4343
					2	4677.5315
1 2	1	3837.2725	2691.0795		1	4677.5866
	0	3837.3210	2691.0934		0	···
2 3	2	5755.5183	4036.5164	5 6	4	···
	1	5755.7606	4036.5766		3	5612.8443
	0	5755.8388	4036.6043		2	5612.9599
					1	5613.0266
3 4	3	7673.2200	5381.7805		0	5613.0535
	2	7673.7540	5381.9394			
	1	7674.0755	5382.0349	6 7	4	6548.0243
	0	7674.1829	5382.0695		3	6548.2119
					2	6548.3478
4 5	4	9590.1474	6726.8470		1	6548.4283
	3	9591.0854	6727.1175		0	6548.4530
	2	9591.7558	6727.3142			
	1	9592.1583	6727.4331	7 8	3	7483.5313
	0	9592.2934	6727.4738		2	7483.6854
					1	7483.7780
5 6	4	···	8072.0455		0	7483.8065
	3	11 508.6618	8072.3778			
	2	11 509.4649	8072.6140			
	1	11 509.9490	8072.7572			
	0	11 510.1110	8072.8049			

because of the small D_{JK} (~2 kHz). They are not included in the table or in the fit. The $J=4\rightarrow5$ transitions for ^{82}Kr–C_6H_6–H_2O and ^{83}Kr–C_6H_6–H_2O were found in predicted regions but they were not cataloged or analyzed. A search for ^{36}Ar–C_6H_6–H_2O was not successful due to its very low (0.34%) natural abundance.

TABLE II. Symmetric top rotational constants determined for the Rg–C_6H_6–H_2O trimers in the $m=0$ state.[a]

Trimer	B (MHz)	D_J (kHz)	D_{JK} (kHz)	σ (kHz)
		Neon		
^{20}Ne–C_6H_6–H_2O	959.3504(1)	2.425(2)	13.385(5)	1.4
^{20}Ne–C_6H_6–HDO	944.4244(1)	2.332(1)	14.925(5)	1.8
^{20}Ne–C_6H_6–D_2O	927.2092(2)	2.237(3)	13.21(2)	0.9
^{20}Ne–C_6H_6–$H_2{}^{18}O$	918.3755(1)	2.146(2)	12.04(1)	1.1
^{22}Ne–C_6H_6–H_2O	921.3840(1)	2.349(1)	12.744(7)	0.8
^{22}Ne–C_6H_6–HDO	907.0947(7)	2.24(3)	13.57(7)	1.3
^{22}Ne–C_6H_6–D_2O	890.6366(3)	2.12(1)	12.62(3)	3.2
		Argon		
Ar–C_6H_6–H_2O	672.7784(2)	0.621(4)	3.96(2)	1.2
Ar–C_6H_6–HDO	662.6071(2)	0.585(3)	4.52(1)	1.3
Ar–C_6H_6–D_2O	650.8974(2)	0.574(3)	3.97(1)	1.2
Ar–C_6H_6–$H_2{}^{18}O$	645.7760(2)	0.556(3)	3.62(2)	1.7
		Krypton		
^{84}Kr–C_6H_6–H_2O	467.7753(1)	0.291(8)	1.919(5)	1.0
^{84}Kr–C_6H_6–HDO	460.4453(1)	0.276(1)	2.107(9)	1.1
^{84}Kr–C_6H_6–D_2O	452.1356(1)	0.2697(6)	1.867(7)	1.2
^{84}Kr–C_6H_6–$H_2{}^{18}O$	449.1324(1)	0.261(1)	1.76(1)	1.5
^{86}Kr–C_6H_6–H_2O	463.3386(1)	0.286(1)	1.884(8)	1.0

[a]The standard deviation of the fit is given in parentheses for the last decimal; σ is the rms value of the residues.

The rotational constants found by fitting the observed frequencies to Eq. (2) are included in Table II. The residues (not given) are within the 2 kHz experimental error. Similar measurements and analyses were made for 13 other H_2O and Rg isotopomers, including several with HDO. For all of them we give only the fitted rotational constants and rms deviations included in Table II. Several trends are apparent in the table, as described in Sec. IV.

b. $m=1$ excited state. The symmetric top spectra exhibited by the $m=0$ state of the trimers show that in them the various isotopic species of H_2O are virtually free to rotate, as was found in the corresponding C_6H_6–H_2O dimers. Our primary objective in observing the $m=1$ state transitions was to determine whether the trimer spectra retain the other dynamic features reported for the dimers.[4,5]

In the dimer studies, $m=1$ transitions were found for the H_2O, D_2O, and $H_2{}^{18}O$ isotopomers but not for the HDO, which has distinguishable H/D nuclei. The difference is attributable to the spin statistics of the homonuclear water species which prohibit relaxation of the excited, high-energy $m=1$ state to the $m=0$ ground state, but allow it for HDO. The current experiments on the trimers also failed to turn up $m=1$ transitions for the HDO species.

Spectra of the $m=1$ state were observed for the three parent isotopic species at low J; the results are listed in Table III. As in the case of C_6H_6–H_2O dimers, it was noted that an independent fit of the $m=1$ transitions to Eq. (1) resulted in a much smaller D_J, even in negative values. This was accommodated in the simultaneous fit of $m=0$ and $m=1$ states by modifying the D_J term in Eq. (1) to read $(D_J - D_{JJm}m^2)$.

TABLE III. Observed frequencies (MHz) of rotational transitions for the parent Rg–C_6H_6–H_2O trimers in the $m=1$ state (Rg=^{20}Ne, ^{40}Ar, or ^{84}Kr).

$J\rightarrow J'$	K	Ne–C_6H_6–H_2O	Ar–C_6H_6–H_2O	Kr–C_6H_6–H_2O
0 1	0	1912.6470	...	...
1 2	−1	3824.2940	2684.5117	...
	0	3825.2963	2684.9146	1868.0138
	1	3837.8851[a]	2691.3505[a]	...
2 3	−2	5734.6690	4026.0870	2801.5093
	−1	5736.3657	4026.7536	2801.7750
	0	5737.9479	4027.3907	2802.0305
	1	5739.1910	4028.1942	2802.3529
	2	5756.6777[a]	4036.9910[a]	2806.8023[a]
3 4	−3	...	...	...
	−2	7646.0507	5368.0829	3735.3135
	−1	7648.3564	5368.9877	3735.6834
	0	7650.5998	5369.8893	3736.0455
	1	7652.4297	5370.7436	3736.4044
	2	7653.8694	5371.3997	3736.6627
	3	7675.2983[a]	5382.5786[a]	3742.3721[a]
4 5	−4		...	...
	−3		6708.8292	...
	−2		6710.0484	4669.1088
	−1		6711.2073	4669.5821
	0		6712.4178	4670.0667
	1		6713.1556	4670.3949
	2		6714.0588	4670.7390
	3		6714.7090	4670.9852
	4		6728.1185[a]	4677.9122[a]

[a]These lines are displaced by some as yet unknown perturbation.

The rotational and centrifugal distortion constants for both $m=0$ and $m=1$ states are given in Table IV.

For $m=1$, Eq. (1) predicts a $K=0$ line that is displaced from the $m=0$, $K=0$ symmetric top lines by the term $2(J+1)D_{Jm}m^2$. Also, it predicts progressions of lines with $|mK|=1,2,\ldots,J$ on each side of the $K=0$ line. Most of these lines were observed for the Rg–C_6H_6–H_2O trimers as well as the C_6H_6–H_2O dimers. However, in all cases, the line with $mK=+J$ was missing and an odd line was observed above the symmetric top lines. This odd line was assigned as the $mK=+J$ line in the $m=1$ progressions of Table III. However, an independent fit of them as $K=0$ gives B and D_J values that are very similar to the symmetric top constants in each case. These results are also included in Table IV.

TABLE V. Observed and fitted deuterium hfs in the $J=0\rightarrow1$ transition for the $m=0$ state of the Ne–C_6H_6–HDO trimer.

$F\rightarrow F'$	Obs. (MHz)	Res. (kHz)	Parameters determined	
1→0	1888.7580	0.5	Line center (MHz)	1888.8402
1→2	0.8306	−1.3	χ_{aa}(D) (kHz)	165.51
1→1	0.8824	0.8	β (deg)	34.2

The sign of m and hence of D_{JKm} is not determined from fitting the spectra. We have arbitrarily chosen m to be positive and D_{JKm} to be negative, so that the $m=1$ progression could be labeled as $K=-J$ to 0 to $+J$ as frequency increases. The standard deviation of the fits to the $m=1$ lines is about 50 kHz, which is 50 times our spectral resolution. However, these are significantly better than the standard deviation for the $m=1$ lines of the dimers (~320 kHz).

2. Nuclear hyperfine structure (hfs)

The deuterium quadrupole and H–H dipole–dipole interactions of the water's isotopic species were useful indicators of its dynamic state in the benzene–water dimer, as described in detail previously.[4] However, these hyperfine interactions are small, of the order of 100 kHz, and we have observed and analyzed the resultant splittings only in the $J=0\rightarrow1$ and $1\rightarrow2$ transitions. For the trimers this has limited our hfs studies to the Ne species ($B=910$ to 960 MHz) and to the Ar $J=1\rightarrow2$ transitions even though the Kr–C_6H_6 interactions are stronger and more likely to affect the dynamic state of the water. In any event, the results outlined below clearly indicate that the state of the water in the trimer does not differ appreciably from that in the dimer, either dynamically or structurally.

a. Ne–C_6H_6–HDO. The most direct information about the dynamic state of the water in the trimer comes from the deuterium ($I=1$) quadrupolar hfs for the HDO isotopomer. The hfs observed in the $J=0\rightarrow1$ transition of

TABLE IV. Rotational constants obtained by a simultaneous fit of the $m=0$ and $m=1$ states for the C_6H_6–H_2O dimer[a] compared with those for the Rg–C_6H_6–H_2O trimers (Rg=^{20}Ne, ^{40}Ar, or ^{84}Kr).

Constant	Units	C_6H_6–H_2O	Ne–C_6H_6–H_2O	Ar–C_6H_6–H_2O	Kr–C_6H_6–H_2O
B	MHz	1994.7735(2)	959.3504(1)	672.7784(2)	467.776 6(2)
D_J	kHz	3.354(1)	2.425(2)	0.621(4)	0.291(8)
D_{JK}		37.91(2)	13.385(5)	3.96(2)	1.919(5)
D_{Jm}	MHz	13.05(7)	3.021(7)	1.529(8)	0.760(3)
D_{JKm}	kHz	−1840(10)	−243(1)	−100(1)	−41.3(5)
H_{JKm}		36(7)	4(1)	2.0(8)	1.1(3)
D_{JJm}		14(3)	2.0(2)	0.25(18)	0.06(6)
$\sigma(m=0)$		1.3	1.4	1.2	1.0
$\sigma(m=1)$		320	58.4	74	28
		Displaced $m=1$, $K=+J$ component[b]			
B	MHz	1995.3856(1)	959.4907(6)	672.8423(3)	467.805 74(3)
D_J	kHz	3.440(2)	2.45(2)	0.612(9)	0.290 0(3)

[a]From Ref. 4.
[b]Fitted as a $K=0$ transition.

Ne–C_6H_6–HDO is given in Table V along with its fit using the basis set $I_D+J=F$.[4,24] The quadrupole coupling constant χ_{aa}(D) found in the fit is 165.5 kHz. It is the projection of χ_0(D) for free HDO onto the **a** axis of the trimer, averaged over its motions,

$$\chi_{aa}(\mathrm{D})=(1/2)\chi_0(\mathrm{D})\langle 3\cos^2\beta-1\rangle, \quad (3)$$

where β is the projection angle between the O–D bond axis and the **a** axis. The χ_0(D) of free HDO is reported to be 315 kHz,[25] leading to a β of 34.2°. The corresponding values for χ_{aa}(D) and β in the dimer[4] are 168.3 kHz and 33.9 deg, differing only slightly and confirming that the benzene–water interaction is monodentate in character with the D preferentially bonded to the benzene aromatic ring.

b. Ne–C_6H_6–H_2O/D_2O. The trimers and dimers with H_2O or D_2O have two identical water nuclei and the total wave function of the species should be antisymmetric (symmetric) with respect to the exchange of the H(D). Thus the parity of the total wave function is determined by the product of the nuclear spin function ψ_n and rotational function ψ_r. In favorable circumstances ψ_n can be found from the hfs or lack of it, and conclusions drawn about the nature of ψ_r.

For the dimer, Gotch and Zwier[9] assumed the water to be freely rotating about its C_2 axis, coaxial with the benzene. Here the dimer belongs to the G_{24} molecular symmetry group for which the isotopomer with $H_2O(D_2O)$ is predicted to have an antisymmetric (symmetric) ψ_n for the $m=0$ state and a symmetric (antisymmetric) ψ_n for the $m=1$ state. The hfs reported[4] for the $m=0$ state of C_6H_6–H_2O/D_2O agrees with these predictions. However, for the $m=1$ state it was found that different spin states were required for the $K=0$ and the $K=\pm1$ levels of each isotopomer.

In the present study the hfs of the trimers, primarily Ne–C_6H_6–H_2O, was found to be consistent with that obtained for the dimers. With the H_2O containing trimer we found no evidence of hfs in transitions of the $m=0$ state or in the $K=0$ transitions of the $m=1$ state, showing that these two protons are in the singlet, antisymmetric spin state $I_H=0$. But the $J=1\rightarrow2$, $K=-1$ and $+1$ transitions for the $m=1$ state, at 3824.294 and 3837.885 MHz, are both close "doublets" with splittings of 17.5 and 14.5 kHz, respectively. They are the strongest hf components ($F=1\rightarrow2$ and $2\rightarrow3$) for the symmetric $I_H=1$ triplet spin state. Virtually identical results were obtained for the $J=1\rightarrow2$, $K=0,\pm1$ transitions of the Ar containing trimer. The doublets have somewhat different splittings of 21.2 and 13.9 kHz in the dimer (Table VIII, Ref. 4). The D_2O containing dimer has hfs in both the symmetric ($I_D=0,2$) and antisymmetric ($I_D=1$) states.[4] It was present as expected however S/N, resolution, and overlap limitations discouraged analysis.

3. Structural analysis

The structural analysis given here for the trimers and in the next section for the Rg–C_6H_6 dimers neglects the effects of intermolecular as well as intramonomer vibrations. This introduces appreciable model error because the potential energy surfaces for the complexes have relatively shallow minima, giving large amplitude intermolecular modes. Corrections for such effects were not attempted so it should be kept in mind that the structural parameters obtained are approximate.

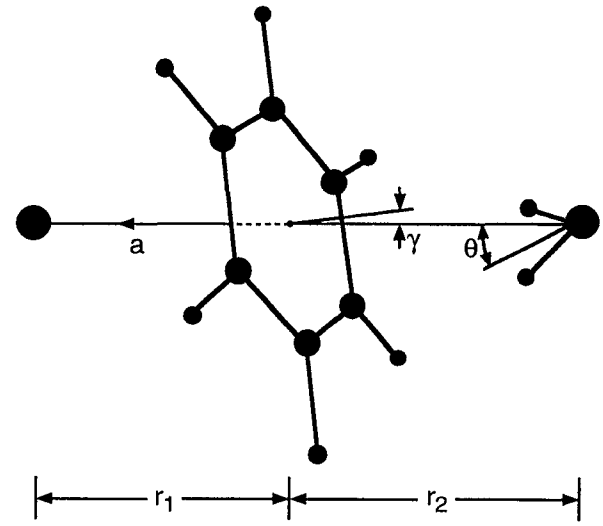

FIG. 2. Molecular geometry and structural parameters used to describe the $m=0$ state of the Rg–C_6H_6–H_2O sandwich trimers. The small barrier to internal rotation of the water makes the trimer behave like a symmetric top.

In analyzing the structures of the trimers we focus on the $m=0$ ground state and treat it as a symmetric top even though, without "free" internal rotation of the H_2O, it is an asymmetric top. As noted above, the trimers may be viewed as composites of the Rg–C_6H_6 and C_6H_6–H_2O dimers, with the same approximate set of structural parameters. These include the Rg to c.m. (C_6H_6) distance r_1, the c.m. (C_6H_6) to c.m. (H_2O) distance r_2, the rms tilt angle γ between the C_6 axis of the benzene and the **a** axis, and the rms angle θ between the C_2 axis of water and the **a** axis, as given in Fig. 2.

An analysis based on isotopic substitution was used to determine most of these parameters for the three trimers, with ^{20}Ne, ^{40}Ar, ^{84}Kr, H_2, and ^{16}O as the parent isotopic species and ^{22}Ne, ^{86}Kr, D_2, and ^{18}O as the species substituted. An attempt was made to observe ^{36}Ar–C_6H_6–H_2O but it was unsuccessful because of the very low natural abundance (~0.34%) of ^{36}Ar. Isotopic substitution of the Rg or O gives its distance a_X along the **a** axis from the c.m. of the trimer to be $\Delta I_b=\mu_s a_X^2$, where $\Delta I_b = I_b' - I_b$ and $\mu_s=M\Delta m/(M+\Delta m)$ is the reduced mass for the substitution.[24]

The ^{18}O substitution gives the oxygen position a_O but for our purposes we need a_{H_2O}, the position of the H_2O c.m. The conversion requires that the orientation (θ) of the H_2O be determined and that the symmetric top behavior of the trimer be addressed. The same problems arose with the C_6H_6–H_2O dimer[4] and the same approximate approach is used here. We treat the H_2O and D_2O as rotors with threefold symmetry. Thereby the substitution of D_2O for H_2O is a multiple off-axis substitution[24] of $\Delta m'=\frac{2}{3}(m_D-m_H)=\frac{2}{3}\Delta m$. This enables us to obtain a_H and b_H from the H_2O/D_2O substitution data with the following relation:

TABLE VI. Structural parameters found for the Rg–C_6H_6–H_2O trimers compared with those in the Rg–C_6H_6 and C_6H_6–H_2O dimers.[a]

Parameters	Units	Ne–C_6H_6–H_2O	Ar–C_6H_6–H_2O	Kr–C_6H_6–H_2O
r_1	Å	3.391	3.554	3.659
δr_1		−0.017	−0.005	−0.004
r_2		3.334	3.332[b]	3.330
δr_2		+0.005	+0.003	+0.001
θ	deg	36.8	37.6	38.4
$\Delta\theta$		0	+0.8	+1.6
γ		22.9	22.3	21.2
$\Delta\gamma$		+2.2	~+4.3	+4.6

[a]The parameters are defined in Fig. 2. The changes in the parameters are those occurring upon trimer formation. Vibrational effects are neglected.
[b]This value was assumed by reference to the results for the Ne and Kr containing trimers in order to get a value for r_1.

$$\Delta I_b = \Delta m b_H^2 + [2\Delta m M/(M+2\Delta m)]a_H^2, \tag{4}$$

where $b_H^2+\Delta a_H^2 = r(OH)^2$. Here r (OH) is the O–H distance in free H_2O and $\Delta a_H = a_O - a_H$ is its projection onto the **a** axis of the trimer.

For example, if the C_2 and C_6 axes of H_2O and C_6H_6 were coincident, Δa_H should be the same as the altitude observed in free H_2O, which is 0.595 Å.[26] For the C_6H_6–H_2O dimer this type of analysis gave Δa_H to be 0.477 Å. It corresponds to a projection angle θ=36.7 deg, the on average angle between the C_2 axis of H_2O and the **a** axis of the axially symmetric dimer. Similar analyses for the trimers gave values for θ of 36.8, 37.6, and 38.4 deg for the Ne, Ar, and Kr species. With values for θ in hand, a_O can be converted to a_{H_2O} by using them to project the O to c.m. (H_2O) distance of 0.0666 Å onto the **a** axis.[4] The value of $a_{C_6H_6}$ can now be determined from a_{Rg} and a_{H_2O} with the first moment condition

$$a_{Rg}m_{Rg} + a_{C_6H_6}m_{C_6H_6} + a_{H_2O}m_{H_2O} = 0. \tag{5}$$

Finally r_1 and r_2 are obtained readily from the three a_X values, giving the results listed in Table VI.

In order to find γ we used the parallel axis theorem to write the following inertial equation for the trimeric symmetric tops:

$$I_b = m_{Rg}a_{Rg}^2 + m_{C_6H_6}a_{C_6H_6}^2 + m_{H_2O}a_{H_2O}^2 + I_b(C_6H_6)\langle 1+\tfrac{1}{2}\sin^2\gamma\rangle + I_0(H_2O)\langle 1+\tfrac{1}{2}\sin^2\theta\rangle. \tag{6}$$

It is similar to that used for the Kr–C_6H_6 dimer[3] but with terms for the H_2O. The symmetric top behavior of H_2O is accommodated by redistributing the H_2 mass with threefold symmetry about the C_2 axis of the H_2O, as in the derivation of Eq. (4). $I_0(H_2O)$ is then the moment of inertia about axes perpendicular to the original C_2 axis. It is small and has little effect on the values of γ, the results for which are also given in Table VI.

TABLE VII. Observed frequencies of rotational transitions for the Ne–C_6H_6 dimers and their fit as symmetric tops.

$J\rightarrow J'$	K	^{20}Ne–C_6H_6 (MHz)	Residue (kHz)	^{22}Ne–C_6H_6 (MHz)	Residue (kHz)
0 1	0	3 620.4346	2.3	a	
1 2	1	7 240.0460	−0.3	6 884.5933	−0.3
	0	7 240.3992	−1.2	6 884.9206	−1.4
2 3	2	10 857.3157	0.1	10 324.3225	−1.1
	1	10 858.9076	0.1	10 325.7999	−1.1
	0	10 859.4397	−0.1	10 326.2949	0.1
3 4	3	14 470.7194	0.1	13 760.4495	0.4
	2	14 474.2448	−0.7	13 763.7257	0.7
	1	14 476.3762	1.6	13 765.7029	1.6
	0	14 477.0856	−0.9	13 766.3640	2.2
4 5	4	b		17 191.5556	−0.3
	3			17 197.2667	0.8
	2			17 201.3769	−1.1
	1			17 203.8573	−0.3
	0			17 204.6876	−0.1
Constant	Units				
B	MHz	1 810.254 8(3)		1 721.375 6(2)	
D_J	kHz	19.344 71(1)		18.136 53(1)	
D_{JK}		88.434 9(2)		82.012 50(5)	
H_{JK}	Hz	−20(6)		−19(1)	
H_{KJ}		70(11)		56(2)	

[a]Obscured by a transition of the benzene dimer.
[b]Above our present frequency range.

B. Rg–C_6H_6 Dimers

Comparative study of the Rg–C_6H_6–H_2O trimer is facilitated by a good data base for the Rg–C_6H_6 and C_6H_6–H_2O dimers. In this section we report our results for the Ne–C_6H_6 dimer and compile corresponding properties for the Ar and Kr containing dimers.

1. Spectra and analysis for Ne–C_6H_6

A search for the J=0→1 transitions of ^{20}Ne–C_6H_6 was based on the ground-state rotational constant reported to be 1808.978 MHz from rotationally resolved UV spectra.[18] The search was lengthened by the weakness of the transition but it was shortly found at 3620.4346 MHz. The higher J symmetric top transitions were then readily observed through J=3→4, limited by the spectrometer range. Also, transitions for the ^{22}Ne isotopic species were observed from J=1→2 through J=4→5. The results are listed in Table VII. Our findings for the ^{20}Ne isotopomer are consistent with those determined by Bauder's group.[21]

Initially Eq. (2), the standard symmetric top equation, was used to fit the observed transitions. But the residues for the J=3→4 and J=4→5 transitions of the two isotopomers were significantly higher (~10 kHz) than the experimental resolution (~1 kHz) clearly indicating a model deficiency. Therefore the higher order terms in H_{JK} and H_{KJ} were included.[24] They improved the fits significantly, giving the residues included in Table VII, which are now within experimental uncertainty.

With the reasonable assumption that the structure of the benzene is not distorted significantly by the weak intermo-

TABLE VIII. Rotational, structural, and potential constants determined for the Rg–C_6H_6 dimers.

Constant	Units	^{20}Ne–C_6H_6 [a]	^{40}Ar–C_6H_6 [b]	^{84}Kr–C_6H_6 [c]
B	MHz	1810.254 8(3)	1181.2595(1)	795.6821(1)
D_J	kHz	19.344 71(1)	3.258(2)	1.325(1)
D_{JK}		88.434 9(2)	17.801(8)	7.895(4)
H_{JK}	Hz	−19(6)	...	...
H_{KJ}		70(10)	...	...
R_0	Å	3.408	3.559	3.663
R_e [d]		3.308	3.520	3.635
R_0-R_e		0.100	0.039	0.028
γ	deg	20.7	~18	16.6
k_s	mdyn/Å	0.008 6	0.0277	0.0349
υ_s	cm^{-1}	30.3	42.2	38.3
ϵ [d]		66	240	324

[a]This research, Table VII.
[b]From Refs. 2 and 3.
[c]From Ref. 3.
[d]Based on a Lennard-Jones 6-12 potential.

lecular forces in the dimer, two parameters are needed to describe the dimer structure. These are the ground-state distance R_0 between the Rg and the c.m. (C_6H_6), and the on average tilt angle γ between R and the sixfold axis of the benzene. In this event, B for the dimer is given by the expression[3]

$$I_b=I_c=I_b(C_6H_6)\langle 1+\tfrac{1}{2}\sin^2\gamma\rangle+\mu_d R^2, \quad (7)$$

where μ_d is the reduced mass of the dimer, treated as pseudodiatomic and $I_b(C_6H_6)$ is reported[27] to be 88.830 087 μÅ^2. If ^{20}Ne/^{22}Ne isotopic substitution has a negligible effect upon R and the tilt angle γ, both parameters can be estimated from the experimental B_0's for the two isotopic species.

This can be done via Eq. (7) by first finding R using a substitution analysis[24] for a_{Ne} and then applying the first moment condition for R. Alternatively, Eq. (7) for the parent (unprimed) species can be subtracted from that for the isotopically substituted (primed) species, giving the following simple equation in R^2:

$$I_b'-I_b=(\mu_d'-\mu_d)R^2. \quad (8)$$

Either method leads to 3.408 Å for R which in turn gives γ=20.7°. In our initial analysis of the Ne–C_6H_6 dimer we did not have the ^{22}Ne–C_6H_6 results.[1] Instead, we neglected the term for γ in Eq. (7) and used the simplified form to determine R. The resulting value of 3.458 Å is significantly longer indicating the importance of the term in $\sin^2\gamma$ in Eq. (7).

2. Comparison of Rg–C_6H_6 dimers

Considerable data are available for the Ar and Kr containing Rg–C_6H_6 dimers. They include not only the rotational and structural constants but also several derived constants related to the potential function, in particular the equilibrium internuclear distance (R_e), the stretching force constant (k_s), the stretching frequency (ν_s), and the well depth (ϵ). These earlier results[2,3] are collected in Table VIII which includes the same set of parameters for Ne–C_6H_6, determined in the same manner.

Although the results were obtained by approximate analyses they provide a semiquantitative picture of the Rg–C_6H_6 potentials. Both the ϵ and R_0-R_e values for Ne–C_6H_6 point to a much shallower and more anharmonic potential surface compared with those for the Ar and Kr containing dimers. The *ab initio* calculations of Hobza *et al.*[13] clearly show this trend which closely parallels the Rg–HCN interaction found for Rg=Ne, Ar, and Kr.[28]

IV. DISCUSSION

The symmetric top rotational spectra and substitution analyses for the Rg–C_6H_6–H_2O trimers establish their structure to be that in which the benzene is sandwiched between the Rg atom and the H_2O molecule with effective axial symmetry. So the trimers can be considered as composites of the Rg–C_6H_6 and C_6H_6–H_2O dimers and one expects any trends in the properties of the trimers upon changing Rg to parallel those for the Rg–C_6H_6 dimer. With this in mind we first review the dimer properties summarized in Table VIII.

The dominant feature of the dimers is the strength of the Rg–benzene interaction, with the experimental well depth ϵ increasing from 66 to 240 to 324 cm^{-1} for Ne, Ar, and Kr. *Ab initio* calculations[13] give systematically larger (3/2) values of 99, 426, and 485 cm^{-1}. In either case, we see that Ar and Kr are quite similar, both having much stronger interactions with benzene than Ne does. This is evident also in D_J, D_{JK}, and k_s. The shallowness of the potential energy surface for Ne–C_6H_6 is shown by the need in it for the H_{JK} and H_{KJ} centrifugal distortion terms. Similar trends are evident for the Rg–HCN dimers.[28] Also, less striking systematics are present in the Rg to c.m. C_6H_6 distance R_0 and in the benzene tilt angle γ.

Trimer formation, as shown by the results summarized in Table VI, has surprisingly little effect upon the four structural parameters ($r_1\gamma;r_2\theta$) of the dimers even though all four are affected systematically by changing Rg in the Ne, Ar, Kr sequence. It is seen that the Rg–C_6H_6 distance r_1 is decreased somewhat in the trimer, the decrease being largest (−0.017 Å) in the case of Ne. On the other hand there is an even smaller *increase* in the C_6H_6–H_2O distance r_2, the increase being largest (+0.005) for Ne. Qualitatively these trends could be attributed to "third-body" effects in which the relatively very strong C_6H_6–H_2O interaction, in the 630 to 1300 cm^{-1} range,[5,10] strengthens the weak Rg–C_6H_6 interaction and is itself affected in the process. Moreover, the weakest Rg–C_6H_6 interaction, that of Ne–C_6H_6, would be affected most.

The angular changes are also systematic, with θ increasing in the Ne→Kr sequence and γ decreasing. The magnitudes of θ and γ are 37 and 21 deg, respectively, indicating large amplitude zero-point bending vibrations. Apparently the benzene "tilt" is reduced by the Rg–C_6H_6 interaction which increases in the Ne→Kr sequence. However, θ is *increased* (H_2O flattened) by the third-body effects of the Rg–C_6H_6 interaction.

In all three trimers the centrifugal distortion constants are much smaller than for the corresponding dimers. The trends shown for Rg–C_6H_6 in Table VIII and for Rg–C_6H_6–H_2O in Table IV are due to strengthening of the

Rg–C_6H_6 interaction as the Rg changes from Ne to Ar to Kr. Also, the change in D_J and D_{JK} for Ne–C_6H_6 as it forms Ne–C_6H_6–H_2O is worth mentioning. For Ne–C_6H_6 the centrifugal distortion constants are large, and even at $J=3$ or 4, higher order terms were needed in fitting the spectra. But for Ne–C_6H_6–H_2O even at $J=8\rightarrow9$ (the highest transitions observable in our instrument) the standard symmetric top equation gives a very good fit. The change in D_J appears to be a good indicator of the additional stabilization of a given dimer by trimer formation. For example, D_J decreases from 3.354 for C_6H_6–H_2O to 2.425 kHz in Ne–C_6H_6–H_2O. However, it changes from 19.345 kHz for Ne–C_6H_6 to 2.425 kHz for Ne–C_6H_6–H_2O even though the increase in mass is roughly the same for the addition of Ne/H_2O.

Several lines of evidence show that axial addition of the Rg has little effect upon the C_6H_6–H_2O structure or on the dynamic state of the water in it. The C_6H_6 to H_2O distance r_2 in the three trimers is the same within model error as in the dimer. Also, the orientation of the H_2O molecule is little affected, the angle θ between its C_2 axis and the **a** axis increasing only by 0, 0.8, and 1.6 deg for Ne, Ar, and Kr. Similarly, the hfs from the water, to the degree that it could be observed, was virtually identical to that reported[4] for the C_6H_6–H_2O dimer. Observations included the H–H hfs in the $J=0\rightarrow1$ and $1\rightarrow2$ transitions of Ne–C_6H_6–H_2O and the $J=1\rightarrow2$ transition of Ar–C_6H_6–H_2O. Attempts to analyze the deuterium quadrupole hfs for the corresponding transitions of the D_2O isotopomers were unsuccessful because of poor S/N. The hfs depends on the spin statistics and symmetry as well as on the dynamic state of the H_2O/D_2O, both aspects of which were confirmed for the H_2O containing trimer. Also confirmed for the trimer and still unexplained is the displacement of the $K=+J$, $m=1$ transitions.

In closing, mention should be made of the rapidly increasing variety of exotic trimers containing a planar aromatic molecule which are being investigated. These include not only the symmetric Ar–C_6H_6–Ar trimer[6,29,30] but an asymmetric conformer as well.[30] Similarly, two stable conformers have been predicted for the furan–Ar_2 trimer by molecular mechanics calculations, one a symmetric sandwich and the other with both argon atoms on the same side of the furan ring.[31] The sandwich form has been identified by its rotational spectrum.

ACKNOWLEDGMENTS

We thank Professor W. Klemperer for fruitful discussions. This material is based on work supported by the National Science Foundation under Grant No. CHE 91-17199. In addition, acknowledgment is made to the Petroleum Research Fund, administered by the American Chemical Society, for partial support of this research.

[1] E. Arunan, T. Emilsson, and H. S. Gutowsky, J. Chem. Phys. **99**, 6208 (1993).
[2] Th. Brupbacher and A. Bauder, Chem. Phys. Lett. **173**, 435 (1990).
[3] T. D. Klots, T. Emilsson, and H. S. Gutowsky, J. Chem. Phys. **97**, 5335 (1992).
[4] H. S. Gutowsky, T. Emilsson, and E. Arunan, J. Chem. Phys. **99**, 4883 (1993).
[5] S. Suzuki, P. G. Green, R. E. Bumgarner, S. Dasgupta, W. A. Goddard III, and G. A. Blake, Science **257**, 942 (1992).
[6] Th. Weber and H. J. Neusser, J. Chem. Phys. **94**, 7689 (1991).
[7] R. S. Ruoff, T. Emilsson, T. D. Klots, C. Chuang, and H. S. Gutowsky, J. Chem. Phys. **89**, 138 (1988).
[8] R. S. Ruoff, T. Emilsson, C. Chuang, T. D. Klots, and H. S. Gutowsky, J. Chem. Phys. **90**, 4069 (1989); **93**, 6363 (1990).
[9] A. J. Gotch and T. S. Zwier, J. Chem. Phys. **96**, 3388 (1992).
[10] J. D. Augspurger, C. E. Dykstra, and T. S. Zwier, J. Phys. Chem. **96**, 7252 (1992).
[11] A. Ben-Naim, *Hydrophobic Interactions* (Plenum, New York, 1980).
[12] G. T. Fraser, F. J. Lovas, R. D. Suenram, D. D. Nelson, Jr., and W. Klemperer, J. Chem. Phys. **84**, 598 (1986).
[13] P. Hobza, O. Bludský, H. L. Selzle, and E. W. Schlag, J. Chem. Phys. **97**, 335 (1992).
[14] Th. Brupbacher, H. P. Lüthi, and A. Bauder, Chem. Phys. Lett. **195**, 482 (1992).
[15] J. Jortner, U. Even, S. Leutwyler, and Z. Berkovitch-Yellin, J. Chem. Phys. **78**, 309 (1983).
[16] H.-Y. Kim and M. W. Cole, J. Chem. Phys. **90**, 6055 (1989).
[17] Th. Weber, A. Von Bargen, E. Riedle, and H. J. Neusser, J. Chem. Phys. **92**, 90 (1990).
[18] Th. Weber, E. Riedle, H. J. Neusser, and E. W. Schlag, J. Mol. Struct. **249**, 69 (1991).
[19] Th. Weber, E. Riedle, H. J. Neusser, and E. W. Schlag, Chem. Phys. Lett. **183**, 77 (1991).
[20] S. M. Beck, M. G. Liverman, D. L. Monts, and R. E. Smalley, J. Chem. Phys. **70**, 232 (1979).
[21] A. Bauder (personal communication).
[22] T. J. Balle and W. H. Flygare, Rev. Sci. Instrum. **53**, 33 (1981); C. Chuang, C. J. Hawley, T. Emilsson, and H. S. Gutowsky, *ibid.* **61**, 1629 (1990).
[23] T. C. Germann, T. Emilsson, and H. S. Gutowsky, J. Chem. Phys. **95**, 6302 (1991).
[24] W. Gordy and R. L. Cook, *Microwave Molecular Spectra*, 3rd ed. (Wiley, New York, 1984).
[25] D. Yaron, K. I. Peterson, D. Zolandz, W. Klemperer, F. J. Lovas, and R. D. Suenram, J. Chem. Phys. **92**, 7095 (1990).
[26] R. L. Cook, F. C. DeLucia, and P. Helminger, J. Mol. Spectrosc. **53**, 62 (1974).
[27] M.-L. Junttila, J. L. Domeneck, G. T. Fraser, and A. S. Pine, J. Mol. Spectrosc. **147**, 513 (1991).
[28] H. S. Gutowsky, J. D. Keen, T. C. Germann, T. Emilsson, J. D. Augspurger, and C. E. Dykstra, J. Chem. Phys. **98**, 6801 (1993).
[29] M. Schmidt, M. Mons, and J. LeCalvé, Chem. Phys. Lett. **177**, 371 (1991).
[30] M. Schmidt, M. Mons, J. LeCalvé, P. Millié, and C. Cossart-Magos, Chem. Phys. Lett. **183**, 69 (1991).
[31] R. M. Spycher, P. M. King, and A. Bauder, Chem. Phys. Lett. **191**, 102 (1992).